

Cosmological Acceleration Through Transition to Constant Scalar Curvature

Leonard Parker¹, William Komp², and Daniel A. T. Vanzella³

*Physics Department, University of Wisconsin-Milwaukee,
Milwaukee, WI 53201, USA*

ABSTRACT

As shown by Parker and Raval, quantum field theory in curved spacetime gives a possible mechanism for explaining the observed recent acceleration of the universe. This mechanism, which differs in its dynamics from quintessence models, causes the universe to make a transition to an accelerating expansion in which the scalar curvature, R , of spacetime remains constant. This transition occurs despite the fact that we set the renormalized cosmological constant to zero. We show that this model agrees very well with the current observed type-Ia supernova (SNe-Ia) data. There are no free parameters in this fit, as the relevant observables are determined independently by means of the current cosmic microwave background radiation (CMBR) data. We also give the predicted curves for number count tests and for the ratio, $w(z)$, of the dark energy pressure to its density, as well as for $dw(z)/dz$ versus $w(z)$. These curves differ significantly from those obtained from a cosmological constant, and will be tested by planned future observations.

Subject headings: cosmic microwave background — cosmological parameters — cosmology: observations — cosmology: theory — gravitation — supernovae: general

1. Introduction

Observational evidence appears increasingly strong that the expansion of the universe is undergoing acceleration that started at a redshift z of order 1 (Riess et al. 1998, 2001;

¹leonard@uwm.edu

²wkomp@uwm.edu

³vanzella@uwm.edu

Perlmutter et al. 1998, 1999). Observations of scores of type-Ia supernovae (SNe-Ia) out to z of about 1.7 support this view (Riess et al. 2001), and even glimpse the earlier decelerating stage of the expansion. It is fair to say that one of the most important questions in physics is: what causes this acceleration?

One of the more obvious possible answers is that we are observing the effects of a small positive cosmological constant Λ (Krauss & Turner 1995; Ostriker & Steinhardt 1995; Dodelson, Gates, & Turner 1996; Colberg et al. 2000). Another, less obvious possibility is that there is a quintessence field responsible for the acceleration of the universe (Caldwell, Dave, & Steinhardt 1998; Zlatev, Wang, & Steinhardt 1999; Dodelson, Kaplinghat, & Stewart 2000; Armendariz-Picon, Mukhanov, & Steinhardt 2001). Quintessence fields are scalar fields with potential energy functions that produce an acceleration of the universe when the gravitational and classical scalar (quintessence) field equations are solved. More recently, Parker & Raval (1999a,b,c, 2000, 2001) showed that a quantized free scalar field of very small mass in its vacuum state may accelerate the universe. Their model differs from any quintessence model in that the scalar field is free, thus interacting only with the gravitational field. The nontrivial dynamics of this model arises from well-defined finite quantum corrections to the action that appear only in curved spacetime. This was the first model to present a realization of dark energy with ratio of pressure to energy density taking values more negative than -1 . Other models having this property have subsequently been proposed (Caldwell 2002; Melchiorri et al. 2002).

The physics of the Parker-Raval model is based on quantum field theory in curved spacetime. The renormalized (i.e., observed) cosmological constant Λ is set to zero. Several mechanisms have been proposed that tend to drive the value of Λ to zero (Dolgov 1983; Ford 1987, 2002; Tsamis & Woodard 1998a,b; Abramo, Tsamis, & Woodard 1999), but these mechanisms play no role in this model. The energy-momentum tensor of the quantized field in its vacuum state is determined by calculating an effective action (Schwinger 1951; DeWitt 1965; Jackiw 1974) in a general curved spacetime. The spacetime is unquantized, and is itself determined self-consistently from the Einstein gravitational field equations involving the vacuum expectation value of the energy-momentum tensor, as well as the classical energy momentum tensor of matter (including cold dark matter) and radiation. In solving the Einstein equations, the symmetries of the FRW spacetime are imposed, but the spacetime is not otherwise taken as fixed, and the initial value constraints of general relativity are satisfied. The acceleration is the result of including in the effective action a non-perturbative term involving the scalar curvature of the spacetime (Parker & Toms 1985a,b,c; Jack & Parker 1985). The minimal effective action that includes this non-perturbative effect and gives the correct trace anomaly of the energy-momentum tensor was used by Parker and Raval. In applying this effective action to the recent expansion of the universe, terms involving more

than two derivatives of the metric were neglected. In this approximation, a solution was proposed in which the universe undergoes a rapid transition from a standard FRW universe dominated by cold dark matter to one containing significant contributions of vacuum energy and pressure. The proposal is that this negative vacuum pressure is responsible for the observed acceleration of the universe. The reaction back of this negative vacuum pressure on the expansion of the universe is such as to cause a rapid transition to an expansion of the universe in which the scalar curvature remains constant. The vacuum pressure and energy density are determined by a single parameter related to the mass of the scalar field. The transition to constant scalar curvature is the result of a rapid growth in the magnitudes of the vacuum pressure and energy density that occurs in this theory when the scalar curvature approaches a particular value, of the order of the square of the mass of the particle associated with the scalar field. The Einstein equations cause a reaction back on the metric such as to prevent further increase in the magnitudes of the vacuum pressure and energy density. (This effect is analogous to Lenz’s law in electromagnetism.)

The essential cosmological features of this model may be described quite simply. For times earlier than a time t_j (corresponding to $z \sim 1$), the universe undergoes the stages of the standard model, including early inflation, and radiation domination followed by domination by cold dark matter. During the latter stage, at time t_j the vacuum energy and (negative) pressure of the free scalar quantized field increase rapidly in magnitude (from a cosmological point of view). The effect of this vacuum energy and pressure is to cause the scalar curvature R of the spacetime to become constant at a value R_j . The spacetime line element is that of an FRW universe:

$$ds^2 = -dt^2 + a(t)^2[(1 - kr^2)^{-1}dr^2 + r^2d\theta^2 + r^2\sin^2\theta d\phi^2], \quad (1)$$

where $k = \pm 1$ or 0 indicates the spatial curvature. By joining at t_j the matter dominated scale parameter $a(t)$ and its first and second derivatives to the solution for $a(t)$ in a constant R universe, one uniquely determines the scale parameter $a(t)$ for times after t_j . This model is known as the vacuum cold dark matter (VCDM) model of Parker and Raval, or as the *vacuum metamorphosis model* (Parker & Raval 1999c) to emphasize the existence of a rapid transition in the vacuum energy density and pressure.

The constant value, R_j , of the scalar curvature is a function of a single new parameter, \bar{m} , related to the mass of the free scalar field. Therefore, the function $a(t)$ for $t > t_j$ is fully determined by \bar{m} . The values of \bar{m} and t_j can be expressed in terms of observables, namely, the present Hubble constant H_0 , the densities Ω_{m0} and Ω_{r0} of the matter and radiation, respectively, relative to the closure density, and the curvature parameter $\Omega_{k0} \equiv -k/(H_0^2 a_0^2)$. (Here $a_0 \equiv a(t_0)$ is the present value of the cosmological scale parameter.) These observables have been determined with reasonably good precision by various measurements that are

independent of the SNe-Ia (Krauss 2000; Freedman et al. 2001; Hu et al. 2001; Huterer & Turner 2001; Turner 2001; Wang, Tegmark, & Zaldarriaga 2002). Therefore, the value of \bar{m} is known to within narrow bounds, independently of the SNe-Ia observations.

The power spectrum of the CMBR depends largely on physical processes occurring long before t_j . The behavior of $a(t)$ in the VCDM model does not significantly differ from that of the standard model until after t_j . Therefore, the predicted power spectrum in the VCDM model differs only slightly from that of the standard model. We calculate the predicted power spectrum of the CMBR in the VCDM model (as described below), and find the range of values of the above observables that give a good fit to the CMBR observations.

From this range of observables, the corresponding range of the parameter \bar{m} follows. Therefore, the prediction of the VCDM model for the magnitude versus redshift curve of the SNe-Ia is completely determined, with no adjustable parameters. We plot the predicted curves (obtained from this range of \bar{m}) for the distance modulus $\Delta(m - M)$ of the SNe-Ia as a function of z . Comparison with the observed data points, as summarized by Riess et al. (2001), shows that a significant subset of predicted curves fit the SNe-Ia data very well, passing within the narrow error bars of each of the binned data points, as well as of the single data point at $z \approx 1.7$.

We also give the curves predicted by the VCDM model for number counts of cosmological objects as a function of z and for the ratio, $w(z)$, of the vacuum pressure to vacuum energy density, as well as for dw/dz versus w (parametrized by z). The predictions of the VCDM model differ significantly from those of the Λ CDM model. Accurate measurements of these quantities out to z of about 2 would be very telling.

The model we consider here is the simplest of a class of models in which a transition occurs around a finite value of z within the range of possible observation. This general class has been studied from a phenomenological point of view by Bassett et al. (2002a,b). They find that the CMBR, large scale structure, and supernova data tend to favor a late-time transition over the standard Λ CDM model. Although they considered only dark-energy equations of state, w , with $w > -1$, their phenomenological analysis can be generalized to include the present VCDM model. In addition, the VCDM model is readily generalized to include a nonzero vacuum expectation value of the low mass scalar field, which could bring w into the range greater than -1 . In the present paper, we are taking the simplest of the possible VCDM (or vacuum metamorphosis) models, so as to introduce no arbitrary parameters into the fit to the supernova data.

2. How Observables Determine \bar{m}

In this section, we explain how the value of \bar{m} is obtained from H_0 , Ω_{k0} , Ω_{m0} , and Ω_{r0} in the VCDM model. (Here, $\Omega_{m0} \equiv \Omega_{\text{cdm}0} + \Omega_{b0}$, where $\Omega_{\text{cdm}0}$ and Ω_{b0} are the present densities of cold dark matter and baryons, respectively, relative to the closure density.) The relation between \bar{m} and these present observables follows from the Einstein equations, the previously described constancy of the scalar curvature $R = R_j$ for $t > t_j$, and continuity of $a(t)$ and its first and second derivatives at time t_j . For our present purposes, we may define the parameter \bar{m} in terms of R_j , namely, by the relation $\bar{m}^2 = R_j$. (At a microscopic level, \bar{m} is proportional to the mass of the free quantized scalar field.)

The trace of the Einstein equations at time t_j is

$$\bar{m}^2 = R_j = 8\pi G\rho_{mj} , \quad (2)$$

where ρ_{mj} is the energy density of the non-relativistic matter present at time t_j . The density and pressure of the dark energy, ρ_v and p_v , respectively, will be taken to be zero at t_j . We make this assumption in order to avoid introducing a second parameter in addition to \bar{m} . It should be noted for future reference that dropping this assumption will introduce another parameter that would affect mainly the behavior of the predicted SNe-Ia curve near the transition time t_j from matter-dominated to constant-scalar-curvature universe. In the present paper, we do not relax this assumption of zero ρ_{vj} and p_{vj} because we find good agreement of the one parameter VCDM model with the current observational data.

For all $t > t_j$, the scalar curvature is taken to remain constant at the value $R_j = \bar{m}^2$. Thus,

$$6[(\dot{a}/a)^2 + (\ddot{a}/a) + k/a^2] = \bar{m}^2 , \quad (3)$$

where dots represent time derivatives. Defining the variable $x \equiv a^2$, this becomes

$$\frac{1}{2}\ddot{x} + k = \frac{1}{6}\bar{m}^2 x . \quad (4)$$

The first integral of this equation is

$$\frac{1}{4}\dot{x}^2 - \frac{1}{12}\bar{m}^2 x^2 + kx = E , \quad (5)$$

where E is a constant.

One of the Einstein equations at time t_j is

$$H_j^2 + k/a_j^2 = (8\pi G/3)\rho_j , \quad (6)$$

where $H_j \equiv \dot{a}(t_j)/a(t_j)$, $a_j \equiv a(t_j)$, and $\rho_j \equiv \rho(t_j)$ is the total energy density at time $t = t_j$. The last equation can be rewritten as

$$\frac{1}{4}\dot{x}_j^2 + kx_j = (8\pi G/3)\rho_j x_j^2, \quad (7)$$

where subscript j refers to quantities at time t_j . Comparing this with equation (5), one finds that

$$E = \left[(8\pi G/3)\rho_j - \frac{1}{12}\bar{m}^2 \right] x_j^2. \quad (8)$$

Using $\rho_j = \rho_{mj} + \rho_{rj}$, where ρ_{rj} is the radiation energy density at time t_j , and equation (2) to eliminate ρ_j and ρ_{mj} from the last expression for E , we find that

$$E = (8\pi G/3)\rho_{rj}x_j^2 + \frac{1}{4}\bar{m}^2x_j^2. \quad (9)$$

Thus, equation (5) gives the following conserved quantity:

$$\frac{1}{4}\dot{x}^2 - \frac{1}{12}\bar{m}^2x^2 + kx = (8\pi G/3)\rho_{rj}x_j^2 + \frac{1}{4}\bar{m}^2x_j^2. \quad (10)$$

This is readily written in terms of $a(t)$ and its derivatives. We have $\dot{x}/x = 2\dot{a}/a \equiv 2H(t)$, and $x_j^2/x(t)^2 = [a_j/a(t)]^4$. Hence, the radiation energy density satisfies

$$\rho_{rj}x_j^2/x(t)^2 = \rho_r(t), \quad (11)$$

and equation (10) is

$$H(t)^2 + k/a(t)^2 = (8\pi G/3)\rho_r(t) + \frac{1}{4}\bar{m}^2[a_j/a(t)]^4 + \frac{1}{12}\bar{m}^2. \quad (12)$$

Solving for $[a_j/a(t)]^4$, we obtain (for $t \geq t_j$),

$$[a_j/a(t)]^4 = \frac{4}{\bar{m}^2} [H(t)^2 + k/a(t)^2 - (8\pi G/3)\rho_r(t)] - \frac{1}{3}. \quad (13)$$

Returning to equation (2), we can now express \bar{m} in terms of the present values of ρ_m , ρ_r , H , and k/a . We have

$$\bar{m}^2 = R_j = 8\pi G\rho_{m0}(a_0/a_j)^3. \quad (14)$$

With equation (13), it follows that

$$\bar{m}^2 = 8\pi G\rho_{m0} \left\{ \frac{4}{\bar{m}^2} [H_0^2 + k/a_0^2 - (8\pi G/3)\rho_{r0}] - \frac{1}{3} \right\}^{-3/4}. \quad (15)$$

Using the expression for the present critical density, $\rho_{c0} = 3H_0^2/(8\pi G)$, equation (15) takes the dimensionless form,

$$m_{H0}^2 = 3\Omega_{m0} \left\{ (4/m_{H0}^2) [1 - \Omega_{k0} - \Omega_{r0}] - \frac{1}{3} \right\}^{-3/4}, \quad (16)$$

where $m_{H0} \equiv \bar{m}/H_0$. This is readily solved numerically for m_{H0}^2 . Alternatively, it can be put into the form of a fourth-order equation for m_{H0}^2 and solved analytically. Using the values $\Omega_{m0} = 0.34_{-0.14}^{+0.46}$ and $H_0 = 65_{+10}^{-16}$ km s⁻¹ Mpc⁻¹ obtained in section 5 from the CMBR power spectrum (see fig. 2), as well as $\Omega_{r0} = 8.33 \times 10^{-5}$ and $\Omega_{k0} = 0$, we find $m_{H0} = 3.26_{+0.10}^{-0.62}$ and $\bar{m} = 4.5_{+0.9}^{-1.7} \times 10^{-33}$ eV. (The uncertainties refer to the 95% confidence level.) Note that the fitting of the CMBR power spectrum alone gives us a wide range for Ω_{m0} and H_0 . In order to further restrict our results (thus being able to make stronger predictions), we will adopt the HST-Key-Project result $H_0 = 72 \pm 8$ km s⁻¹ Mpc⁻¹ (Freedman et al. 2001) as a constraint. This narrows the range of our cosmological parameters down to $\Omega_{m0} = 0.34_{-0.14}^{+0.08}$ and $H_0 = 65_{+10}^{-1}$ km s⁻¹ Mpc⁻¹, as can be seen from figure 2. Aiming at combining these two methods of determining the uncertainties of our results, hereafter we adopt the notation exemplified by $\Omega_{m0} = 0.34_{-0.14}^{+(0.46;0.08)}$ and $H_0 = 65_{+10}^{-(16;1)}$ km s⁻¹ Mpc⁻¹, where the uncertainties appearing in parenthesis refer to the 95% confidence level, without and with the HST constraint, respectively. (The sign appearing in front of the parenthesis is common to both uncertainties.) Thus, returning to the parameters m_{H0} and \bar{m} , we have:

$$m_{H0} = 3.26_{+0.10}^{-(0.62;0.08)} \quad (17)$$

and

$$\bar{m} = 4.52_{+0.84}^{-(1.76;0.18)} \times 10^{-33} \text{ eV} . \quad (18)$$

Finally, the solution to equation (4) for $x(t) = a(t)^2$ is

$$\begin{aligned} a(t)^2/a_0^2 &= \cosh \left(\frac{\bar{m}}{\sqrt{3}}(t - t_0) \right) \\ &+ \frac{2\sqrt{3}}{m_{H0}} \sinh \left(\frac{\bar{m}}{\sqrt{3}}(t - t_0) \right) \\ &- \frac{6\Omega_{k0}}{m_{H0}^2} \cosh \left(\frac{\bar{m}}{\sqrt{3}}(t - t_0) \right) + \frac{6\Omega_{k0}}{m_{H0}^2} . \end{aligned} \quad (19)$$

It then follows from $(1/2)\dot{x}(t)/x(t) = H(t)$, that

$$\begin{aligned} H(t)/H_0 &= a(t)^{-2}a_0^2 \left[\cosh \left(\frac{\bar{m}}{\sqrt{3}}(t - t_0) \right) \right. \\ &\left. + \sqrt{3} \left(\frac{m_{H0}}{6} - \frac{\Omega_{k0}}{m_{H0}} \right) \sinh \left(\frac{\bar{m}}{\sqrt{3}}(t - t_0) \right) \right] . \end{aligned} \quad (20)$$

From equations (12), (14), and (16) one obtains the following expression in terms of the redshift, $z \equiv a_0/a - 1$:

$$H(z)^2/H_0^2 = (1 - \Omega_{k0} - m_{H0}^2/12)(1+z)^4 + \Omega_{k0}(1+z)^2 + m_{H0}^2/12 . \quad (21)$$

From equations (14) and (17) one finds the redshift z_j at time t_j ,

$$z_j = [m_{H0}^2/(3\Omega_{m0})]^{1/3} - 1 = 1.19_{+0.47}^{-(0.76;0.19)} . \quad (22)$$

Moreover, from equation (21) we can obtain the redshift, z_a , at which the expansion of the Universe starts to accelerate. In fact, by looking at the deceleration parameter,

$$q \equiv -\frac{a\ddot{a}}{\dot{a}^2} = (1+z) [\ln(H/H_0)]' - 1 , \quad (23)$$

where the prime sign stands for derivative with respect to z , we have that z_a satisfies

$$(1+z_a)H'(z_a) = H(z_a) . \quad (24)$$

Thus, from equation (21) and the cosmological parameters mentioned above, we obtain for the spatially flat VCDM model

$$z_a = \left[\frac{m_{H0}^2/12}{1 - \Omega_{k0} - m_{H0}^2/12} \right]^{1/4} - 1 = 0.67_{+0.35}^{-(0.59;0.15)} . \quad (25)$$

This value is similar to the one obtained using the spatially flat Λ CDM model with $\Omega_{\Lambda 0} = 0.67$:

$$z_{a\Lambda\text{CDM}} \approx \left(\frac{2\Omega_{\Lambda 0}}{1 - \Omega_{\Lambda 0}} \right)^{1/3} - 1 \approx 0.60 . \quad (26)$$

3. The Dark Energy

In the VCDM model, the dark energy is the energy of the vacuum, denoted by ρ_v . This vacuum energy is not in the form of real particles, but may be thought of as energy associated with fluctuations (or virtual particles) of the quantized scalar field. Vacuum energy, ρ_v , and pressure, p_v , must be included as a source of gravitation in the Einstein equations. Thus, for $t > t_j$, one has

$$H(t)^2 + k/a(t)^2 = (8\pi G/3) [\rho_r(t) + \rho_m(t) + \rho_v(t)] . \quad (27)$$

The vacuum energy and pressure remain essentially zero until the time t_j when the value of the scalar curvature R has fallen to a value slightly greater than \bar{m}^2 . Then in a short

time (on a cosmological scale), the vacuum energy and pressure grow, and through their reaction back cause the scalar curvature to remain essentially constant at a value just above $R_j = \bar{m}^2$ (Parker & Raval 1999a,b). Intuitively, this reaction back may be thought of as similar to what happens in electromagnetism when a bar magnet is pushed into a coil of wire. The current induced in the coil produces a magnetic field that opposes the motion of the bar magnet into the coil (Lenz's Law). Similarly, in the present case, the matter dominated expansion of the universe causes the scalar curvature to decrease. But as it approaches the critical value, \bar{m}^2 , the quantum contributions to the energy-momentum tensor of the scalar field grow large in such a way as to oppose the decrease in R that is responsible for the growth in quantum contributions. The universe continues to expand, but in such a way as to keep R from decreasing further.

Defining t_j as the time at which ρ_v and p_v begin to grow significantly, we have to good approximation, equation (2). Evolving ρ_{m_j} forward in time, then gives

$$8\pi G\rho_m(t) = \bar{m}^2 [a_j/a(t)]^3 . \quad (28)$$

One then finds from equation (27) and equation (12) that the vacuum energy density evolves for $t > t_j$ as

$$\rho_v(t) = \frac{\bar{m}^2}{32\pi G} \{1 - 4 [a_j/a(t)]^3 + 3 [a_j/a(t)]^4\} . \quad (29)$$

The conservation laws for the total energy density and pressure and for the energy densities and pressures of the radiation alone and of the matter alone, then imply that ρ_v and the vacuum pressure, p_v , also satisfy the conservation law. It follows that

$$\begin{aligned} p_v(t) &= -\frac{d}{dt}(\rho_v a^3) / \frac{d}{dt}(a^3) \\ &= \frac{\bar{m}^2}{32\pi G} \{-1 + [a_j/a(t)]^4\} . \end{aligned} \quad (30)$$

At late times, as $a_j/a(t)$ approaches zero, one sees that the vacuum energy density and pressure approach those of a cosmological constant, $\Lambda = \bar{m}^2/4$. But at finite times, their time evolution differs from that of a cosmological constant.

One immediately sees from equations (28) and (29) that for $t > t_j$,

$$\rho_v(t) + \rho_m(t) = \frac{\bar{m}^2}{32\pi G} \{1 + 3 [a_j/a(t)]^4\} . \quad (31)$$

Using equation (30), it now follows that

$$p_v(t) = (1/3) [\rho_v(t) + \rho_m(t)] - \bar{m}^2/(24\pi G) . \quad (32)$$

Since $p_m = 0$, and $p_r = (1/3)\rho_r$, the total pressure, p , and energy density, ρ , satisfy the equation of state (Parker & Raval 2000)

$$p(t) = (1/3)\rho(t) - \bar{m}^2/(24\pi G) . \quad (33)$$

From this equation of state and the conservation law, which can be written in the form, $d(\rho a^3)/da + pd(a^3)/da = 0$, we find that for $t > t_j$,

$$\rho(a) = \left(\rho_j - \frac{\bar{m}^2}{32\pi G} \right) (a_j/a)^4 + \frac{\bar{m}^2}{32\pi G} . \quad (34)$$

As the vacuum energy density is taken as zero at $t = t_j$, we have $\rho_j = \rho_{mj} + \rho_{rj} = \rho_{m0}a_0^3/a_j^3 + \rho_{r0}a_0^4/a_j^4$, and then, from equation (14),

$$\rho_j = \bar{m}^2/(8\pi G) + \rho_{r0} [\bar{m}^2/(8\pi G\rho_{m0})]^{4/3} . \quad (35)$$

Then, with equation (28) and (for $t > t_j$) $(a_j/a)^4 = (a_0/a)^4(8\pi G\rho_{m0}/\bar{m}^2)^{4/3}$, equation (34) finally becomes

$$\rho(a) = [\rho_{m0} (3\Omega_{m0}/m_{H0}^2)^{1/3} + \rho_{r0}] (a_0/a)^4 + \bar{m}^2/(32\pi G) . \quad (36)$$

This expression will be used in the next section to calculate, among other things, the age of the Universe as predicted by the Λ CDM model.

4. Age of the universe

The values of t_j and t_0 are found by integration:

$$t = \int_0^t dt = \int_0^{a(t)} da a^{-1} H(a)^{-1} . \quad (37)$$

From equation (27),

$$t = \int_0^{a(t)} da a^{-1} \left\{ -k/a^2 + (8\pi G/3) [\rho_r(a) + \rho_m(a) + \rho_v(a)] \right\}^{-1/2} , \quad (38)$$

This integral is conveniently split in two at time t_j , and expressed in terms of variable of integration $y \equiv a/a_0$:

$$t_j = (H_0)^{-1} \int_0^{a_j/a_0} dy (\Omega_{k0} + \Omega_{m0}y^{-1} + \Omega_{r0}y^{-2})^{-1/2} , \quad (39)$$

and from equation (36),

$$t_0 - t_j = (H_0)^{-1} \int_{a_j/a_0}^1 dy \left\{ \Omega_{k0} + [\Omega_{m0} (3\Omega_{m0}/m_{H0}^2)^{1/3} + \Omega_{r0}] y^{-2} + (m_{H0}^2/12) y^2 \right\}^{-1/2}. \quad (40)$$

Another interesting parameter to obtain is t_a , the time when the expansion of the Universe starts to accelerate:

$$t_0 - t_a = (H_0)^{-1} \int_{a_a/a_0}^1 dy \left\{ \Omega_{k0} + [\Omega_{m0} (3\Omega_{m0}/m_{H0}^2)^{1/3} + \Omega_{r0}] y^{-2} + (m_{H0}^2/12) y^2 \right\}^{-1/2}, \quad (41)$$

where $a_a \equiv a(t_a)$.

Using the cosmological parameters obtained in section 5 by fitting the VCDM model to the CMBR power spectrum data, we have (see eqs. [22] and [25]) $a_j/a_0 = (1 + z_j)^{-1} = 0.46_{-0.08}^{+(0.24;0.04)}$ and $a_a/a_0 = (1 + z_a)^{-1} = 0.60_{-0.10}^{+(0.32;0.06)}$, and consequently, $H_0 t_j = 0.354_{-0.011}^{+(0.084;0.009)}$, $H_0 t_a = 0.535_{-0.017}^{+(0.126;0.013)}$, and $H_0 t_0 = 0.99_{+0.16}^{-(0.26;0.07)}$. Thus, using the correspondent values of H_0 , we finally obtain

$$t_j = 5.33_{-0.84}^{+(3.41;0.22)} \text{ Gyr}, \quad (42)$$

$$t_a = 8.0_{-1.2}^{+(5.2;0.4)} \text{ Gyr}, \quad (43)$$

and

$$t_0 = 14.9 \mp 0.8 \text{ Gyr}. \quad (44)$$

Note that the uncertainty in t_0 is independent of whether or not we adopt the HST-Key-Project result as a constraint. This is because the dependence of t_0 on H_0 and Ω_{m0} is such that the 95% confidence region shown in figure 2 happens to be stretched along lines of constant values of t_0 . The same is true for the Λ CDM model, as discussed by Knox, Christensen, & Skordis (2001).

We can compare the values presented in equations (43) and (44) with the respective ones given by the spatially flat Λ CDM model. Using $\Omega_{\Lambda 0} = 0.67$, the Λ CDM model gives $H_0 t_a \approx 0.536$ and $H_0 t_0 \approx 0.938$. With the best-fit value of the Hubble constant obtained for our model, $H_0 = 65 \text{ km s}^{-1} \text{ Mpc}^{-1}$ (see section 5), this gives $t_a \approx 8.1 \text{ Gyr}$ and $t_0 \approx 14.1 \text{ Gyr}$. Therefore, we see that the age attributed to the Universe by the VCDM model is larger than the age predicted by the Λ CDM model, for essentially the same values of Ω_{m0} and H_0 .

5. Fit to the CMBR power spectrum

In view of recent CMBR observations (Pryke et al. 2002; Masi et al. 2002; Netterfield et al. 2002; Abroe et al. 2001), there is a need to reexamine the results obtained by Parker &

Raval (2001). In this section, we will obtain the cosmological parameters $\omega_{\text{cdm}0} \equiv \Omega_{\text{cdm}0}h^2$, $\omega_{b0} \equiv \Omega_{b0}h^2$, and $H_0 \equiv 100h \text{ km s}^{-1} \text{ Mpc}^{-1}$ which give the best fit of the spatially flat Λ CDM model to the recent measurements of the CMBR power spectrum by Boomerang, MAXIMA, and DAS1 (h is a dimensionless quantity defined by the latter expression). As we have seen, these parameters are the essential ingredients necessary to fix the parameter \bar{m} . [The other necessary parameter, $\Omega_{r0} = 8.33 \times 10^{-5}$, is independently obtained from the CMBR mean temperature and the number of relic neutrino species (Peebles 1993).]

In order to obtain the CMBR power spectrum fluctuations predicted by the Λ CDM model, with given values of $\omega_{\text{cdm}0}$, ω_{b0} , and H_0 , we use a slightly modified version of the CMBFAST⁴ computer code (Seljak & Zaldarriaga 1996; Zaldarriaga & Seljak 2000). The modifications made in the code, described by Parker & Raval (2001), consist of adding the vacuum contributions, ρ_v and p_v , to the total energy density and pressure, respectively, for time $t > t_j$, i.e., after the transition to dark energy dominated epoch.

We set up the CMBFAST code to generate a numerical grid in the 3 dimensional cosmological parameter space ($\omega_{\text{cdm}0}$, ω_{b0} , H_0). We introduce prior information on the value of the present day Hubble constant, H_0 , to be in the range from 45 to 80 with units of $\text{km Mpc}^{-1} \text{ s}^{-1}$. Also, we set the value of the cosmological constant, Λ , to be zero. To perform our numerical analysis consistent with these priors, we generated a class of Λ CDM models with the following cosmological parameters and resolutions (in the form of “initial value” : “final value” : “step size”): $\omega_{b0} = (0.005 : 0.030 : 0.001)$, $\omega_{\text{cdm}0} = (0.05 : 0.31 : 0.01)$, and $H_0 = (45.0 : 80.0 : 1.0) \text{ km s}^{-1} \text{ Mpc}^{-1}$. We chose to vary these three parameters based on the fact that they determine directly \bar{m} , which is the one free parameter of the Λ CDM model. All models generated use the Radical Compression Data Analysis Package⁵ (RadPack) (Bond, Jaffe, & Knox 2000) to compute a χ^2 test statistic that compares the predicted CMBR spectrum to the experimental measurements of DAS1 (Pryke et al. 2002), Boomerang (Masi et al. 2002; Netterfield et al. 2002), and MAXIMA (Abroe et al. 2001) at particular multipoles l . We look for minima of χ^2 in the class of cosmologies specified above. The particular Λ CDM model described by the parameters which give the minimum of χ^2 in our parameter space is called the best fit model.

For the best fit Λ CDM model, we found $\omega_{b0} = 0.022$, $\omega_{\text{cdm}0} = 0.12$, and $H_0 = 65.0 \text{ km s}^{-1} \text{ Mpc}^{-1}$. This best fit has $\chi^2 = \chi^2_{\text{min}} = 48.84$, corresponding to a significance level $\alpha(\chi_{\text{min}}) \equiv \int_{\chi_{\text{min}}}^{\infty} f(\chi^2, n) d(\chi^2) = 0.187$, where $f(\chi^2, n) = [2\Gamma(n/2)]^{-1} (\chi^2/2)^{n/2-1} e^{-\chi^2/2}$ is the χ^2 probability density function (pdf) for n degrees of freedom (the recent CMBR data

⁴<http://physics.nyu.edu/matiasz/CMBFAST/cmbfast.html>

⁵<http://bubba.ucdavis.edu/~knox/radpack.html>

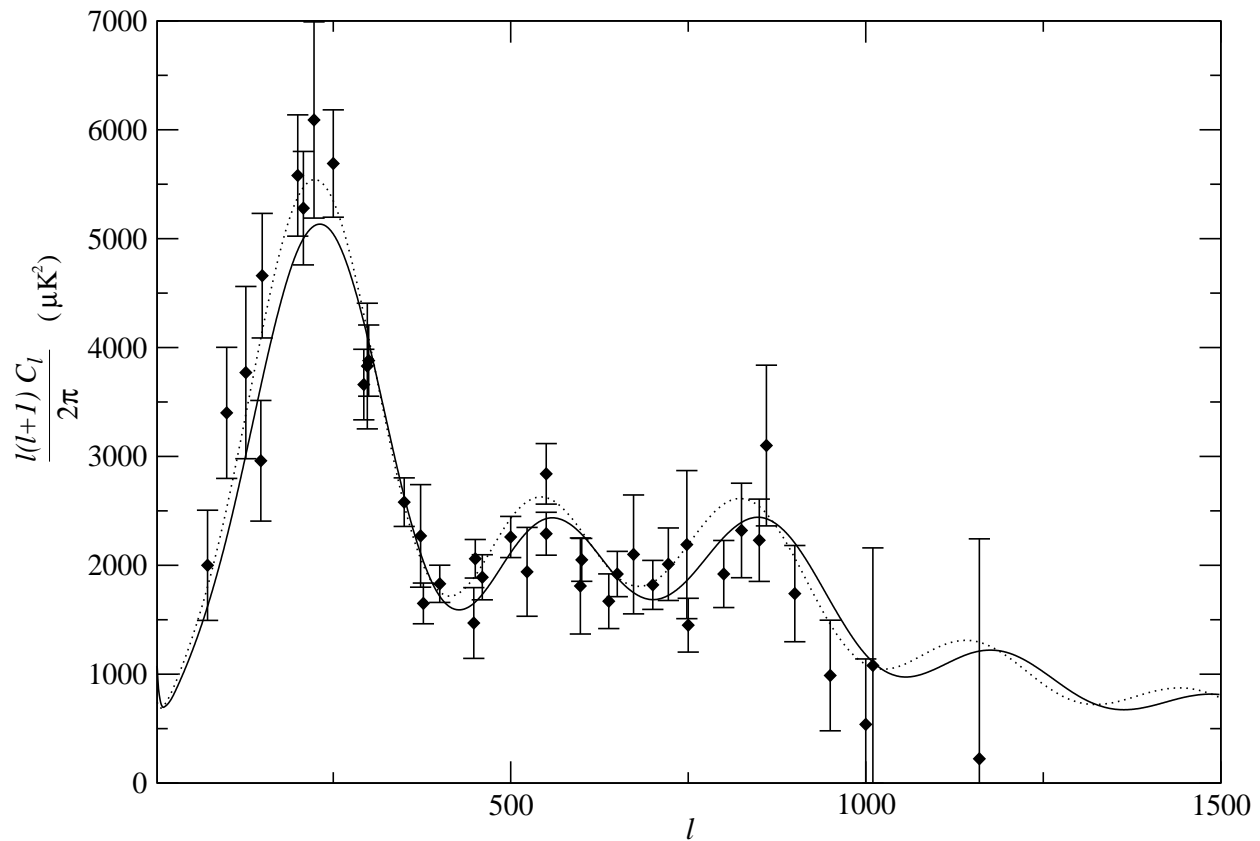


Fig. 1.— Plot of the best fit CMBR power spectrum for the spatially flat VCDM model (solid curve) and of the CMBR power spectrum for the spatially flat Λ CDM model with $\Omega_{\Lambda 0} = 0.67$ (dashed curve). The diamond points and error bars correspond to DASI, Boomerang, and MAXIMA experimental data.

we consider are constituted of 41 experimental points). The three best fit cosmological parameters of the Λ CDM model are similar to the values obtained from the Λ CDM model fit to the CMBR power spectrum (Pryke et al. 2002; Abroe et al. 2001; Masi et al. 2002; Netterfield et al. 2002).

To find the 95% confidence region of our parameter space, we compute the quantity $\chi_{95\%}^2$ where $\alpha(\chi_{95\%}) = 0.05$, and then look for the subset of VCDM models with $\chi^2 \leq \chi_{95\%}^2$ which lie in the parameter space given above. The results for the VCDM model are $H_0 = 65_{-10}^{+16}$ km s⁻¹ Mpc⁻¹, $\omega_{\text{cdm}0} = 0.12_{-0.03}^{+0.06}$, and $\omega_{b0} = 0.022_{-0.004}^{+0.003}$. The uncertainties given above are obtained from the extrema of the 95% confidence region. The range of ω_{b0} is consistent with Big Bang Nucleosynthesis (Bean, Hansen, & Melchiorri 2002), and the best fit value for H_0 lies within the range given by the HST Key Project (Freedman et al. 2001).

From the 95% confidence region in the parameter space ($\omega_{\text{cdm}0}$, ω_{b0} , H_0) we can obtain the 95% confidence region in the space (Ω_{m0} , H_0), recalling that $\Omega_{m0} = (\omega_{\text{cdm}0} + \omega_{b0})/h^2$ and $h \equiv H_0 / (100 \text{ km s}^{-1} \text{ Mpc}^{-1})$. This confidence region is presented in figure 2 (dark-gray region). The reason to concentrate in the parameter space (Ω_{m0} , H_0) is that all quantities we are interested in (e.g., the age of the Universe, the luminosity distances of SNe-Ia, number count tests, the dark energy equation of state) depend directly on Ω_{m0} , not on $\omega_{\text{cdm}0}$ and ω_{b0} separately (except, obviously, the quantities directly related to the CMBR power spectrum). From figure 2 we see that $\Omega_{m0} = 0.34_{-0.14}^{+0.46}$. This very wide range is just a consequence of the fact that the Hubble constant H_0 is not tightly constrained by the CMBR power spectrum. However, adopting the HST-Key-Project result $H_0 = 72 \pm 8$ km s⁻¹ Mpc⁻¹ as a constraint (light-gray region in fig. 2), the acceptable range of Ω_{m0} can be narrowed down to $\Omega_{m0} = 0.34_{-0.14}^{+0.08}$, which then allows us to make stronger predictions about the cosmological quantities mentioned above. Using the even stronger prior $H_0 = 65$ km s⁻¹ Mpc⁻¹ (the best-fit value) we obtain the “best-fit range” $\Omega_{m0} = 0.34 \pm 0.06$, which will be used in the next section to fit (with no free parameters) the luminosity distances of SNe-Ia.

For the CMBR power spectrum predicted by the best fit flat VCDM model (see fig. 1), the multipole numbers l and power intensities $I_l \equiv l(l+1)C_l/(2\pi)$ of the first three peaks and two troughs are given in table 1. The uncertainties Δl and ΔI_l correspond to the 95% confidence region of $\omega_{\text{cdm}0}$, ω_{b0} , and H_0 . Comparing the values given in table 1 with the correspondent results presented by Durrer, Novosyadlyj, & Apunevych (2001), we see that our values for the first three peaks and two troughs are well within the (1σ) ranges for these quantities that can be obtained, in a model-independent way, from the combined Boomerang, MAXIMA, and DASIA data. For instance, the last two columns of table 2 of Durrer, Novosyadlyj, & Apunevych (2001) give the multipole number and the power intensity of the first peak to be $l_{p1} = 213_{-59}^{+35}$ and $I_{p1} = 5041_{-1196}^{+1017}$ μK^2 , respectively.

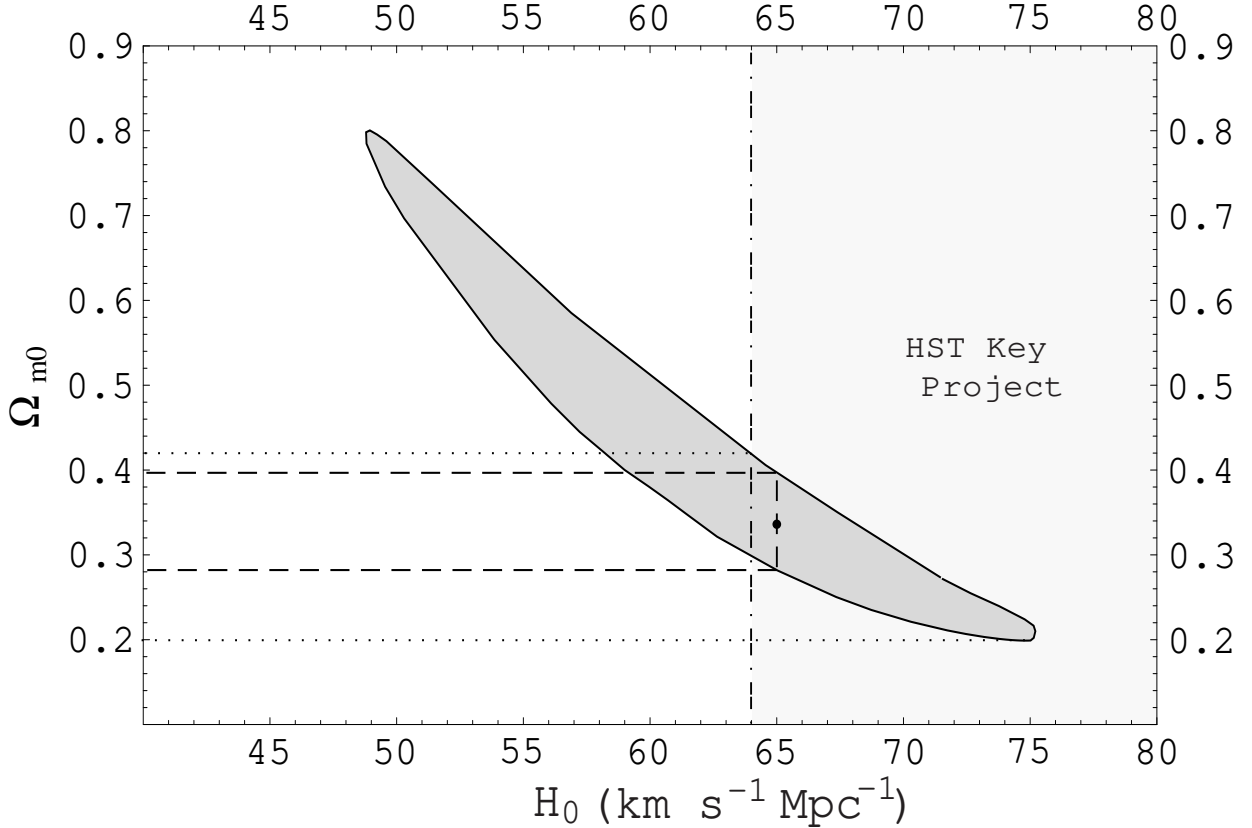


Fig. 2.— Plot of the 95% confidence level (dark-gray region) in the parameters Ω_{m0} and H_0 obtained by fitting the CMBR power spectrum using the Λ CDM model. The extrema of this region, together with the best-fit values, define the ranges $\Omega_{m0} = 0.34^{+0.46}_{-0.14}$ and $H_0 = 65^{+16}_{-10}$ km s $^{-1}$ Mpc $^{-1}$. Adopting the HST-Key-Project result ($H_0 = 72 \pm 8$ km s $^{-1}$ Mpc $^{-1}$, represented by the light-gray region), the range in Ω_{m0} is narrowed down to $\Omega_{m0} = 0.34^{+0.08}_{-0.14}$ (dotted lines). Fixing $H_0 = 65$ km s $^{-1}$ Mpc $^{-1}$, we have $\Omega_{m0} = 0.34 \pm 0.06$ (dashed lines).

The results of this section show that the Λ CDM model gives a reasonable fit to the CMBR power spectrum with values of $\omega_{\text{cdm}0}$, ω_{b0} , and H_0 that are consistent with current observations. The future of CMBR observations looks very promising with a mixture of ground based interferometers (DASI), airborne interferometers (MAXIMA and Boomerang), and satellite experiments (Microwave Anisotropy Probe and the Planck satellite) that will further probe the CMBR anisotropies at higher and lower multipoles.

6. No-parameter fit to the SNe-Ia data

In the present section we compare the luminosity distance as a function of redshift predicted by the Λ CDM model to the measured values of the luminosity distances of SNe-Ia as summarized by Riess et al. (2001). Because all the relevant parameters of the model are determined by fitting the CMBR power spectrum (see sec. 5), this comparison is a no-parameter fit of the Λ CDM model to the SNe-Ia data.

We start by computing the luminosity distance as a function of redshift, $d_L(z)$. As a consequence of equation (1), the comoving coordinate distance $r(z)$ of objects observed with redshift z satisfies

$$\frac{dr}{\sqrt{1 - kr^2}} = \frac{dt}{a(t)} = \frac{dz}{a_0 H(z)}, \quad (45)$$

which leads to

$$r(z) = \begin{cases} \int_0^z [a_0 H(z')]^{-1} dz' & , k = 0 \\ \left(a_0 H_0 \Omega_{k0}^{1/2}\right)^{-1} \sinh\left(H_0 \Omega_{k0}^{1/2} \int_0^z H(z')^{-1} dz'\right) & , k \neq 0 \end{cases}, \quad (46)$$

where $H(z)$ for the Λ CDM model is given by (see eq. [21])

$$\frac{H(z)}{H_0} = \begin{cases} [(1 - \Omega_{k0} - m_{H0}^2/12)(1+z)^4 + \Omega_{k0}(1+z)^2 + m_{H0}^2/12]^{1/2} & , z < z_j \\ [\Omega_{r0}(1+z)^4 + \Omega_{m0}(1+z)^3 + \Omega_{k0}(1+z)^2]^{1/2} & , z \geq z_j \end{cases}. \quad (47)$$

The luminosity distance and the distance modulus are defined respectively as

$$d_L(z) \equiv a_0 (1+z) r(z) \quad (48)$$

and

$$\Delta(m - M)(z) \equiv 5 \log\left(\frac{d_{L1}(z)}{d_{L2}(z)}\right), \quad (49)$$

where d_{L1} is the luminosity distance in the spatially flat Λ CDM model and d_{L2} is the luminosity distance in an arbitrary fiducial model used as normalization. We will set d_{L2} as

Table 1. Multipole numbers l and associated power intensities I_l of the first few peaks and troughs of the CMBR spectrum predicted by the spatially flat VCDM model (see fig. 1). The uncertainties Δl and ΔI_l are calculated from the χ^2 test statistic.

	l	Δl	I_l (μK^2)	ΔI_l (μK^2)
Peaks	230	± 1	5133	+22/−337
	558	+7/−5	2436	+162/−123
	848	+4/−9	2441	+291/−229
Troughs	427	+2/−7	1591	+132/−81
	700	+7/−20	1685	+173/−158

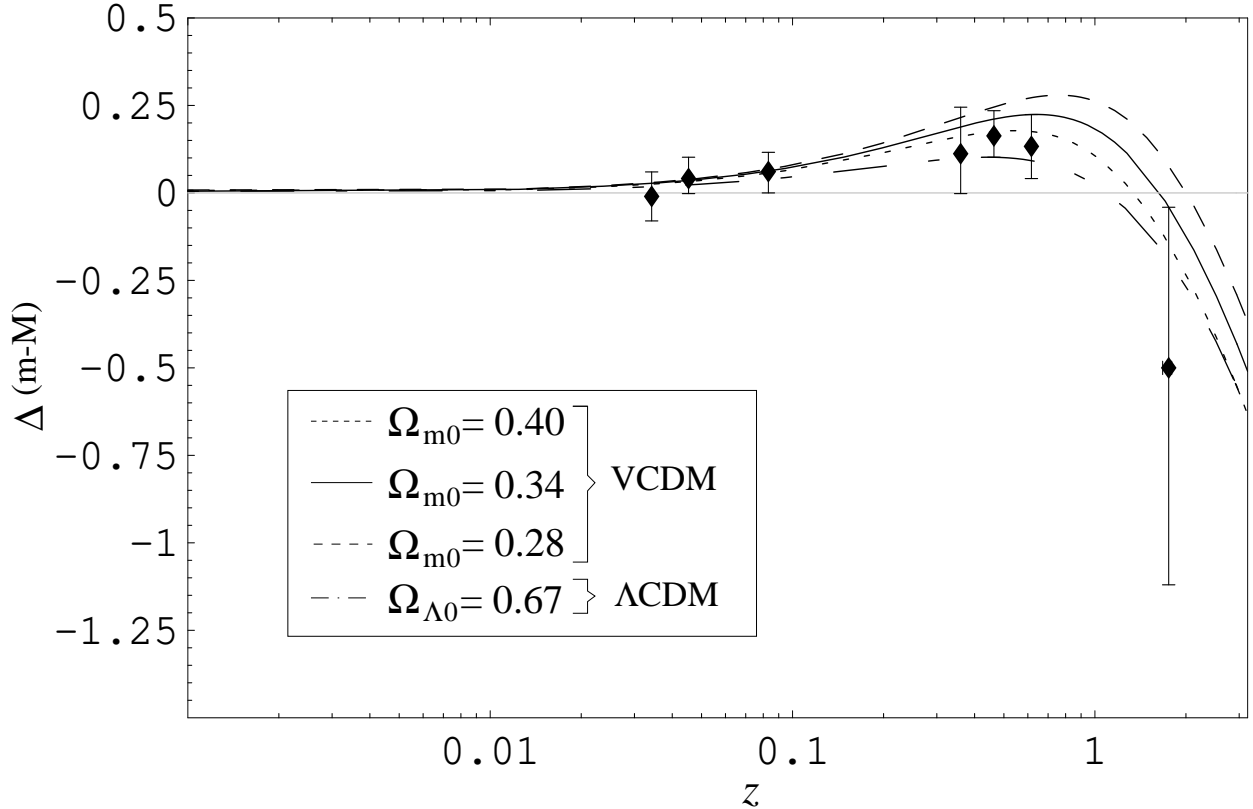


Fig. 3.— Plot of the type-Ia supernovae distance modulus (normalized to a spatially open and empty cosmos) as a function of redshift z for the spatially flat VCDM (with $\Omega_{m0} = 0.34 \pm 0.06$) and Λ CDM (with $\Omega_{\Lambda 0} = 0.67$) models.

the luminosity distance in an open and empty Universe [$a(t) = t$ and $k = -1$], which is the convention used by Riess et al. (2001).

It is important to note that the expression for $\Delta(m - M)$ does not depend explicitly on the present value of the Hubble constant H_0 . However, if we adopt the results of the previous section summarized in figure 2, then fixing different values of H_0 in that figure lead to different 95%-confidence-level ranges for Ω_{m0} , which in turn give rise to different predictions for the SNe-Ia luminosity distances. In particular, using for H_0 the best-fit value $H_0 = 65 \text{ km s}^{-1} \text{ Mpc}^{-1}$ gives us $\Omega_{m0} = 0.34 \pm 0.06$ (see fig. 2). In figure 3 we plot the distance modulus as a function of redshift predicted by the Λ CDM model using this “best-fit range” for Ω_{m0} , as well as the observed distance moduli of SNe-Ia. It can be seen from figure 3 that fixing the values of Ω_{m0} and H_0 that best fit the CMBR data also gives a very good no-parameter fit to the SNe-Ia data. Moreover, any value of Ω_{m0} in the “best-fit range” $\Omega_{m0} = 0.34 \pm 0.06$ gives a reasonably good fit to the SNe-Ia data, as shown by the dashed curves in figure 3. We also show in figure 3 the distance modulus predicted by the Λ CDM model with $\Omega_{\Lambda 0} = 0.67$. We see that even though the predictions of both models differ significantly in the range $0.5 \lesssim z \lesssim 1.5$, current data are still not able to make a clear distinction between them.

More numerous and accurate data on SNe-Ia luminosity distance are expected for the near future. The planned Supernova Acceleration Probe (SNAP)⁶, for instance, aims at cataloging up to 2,000 SNe-Ia per year in the redshift range $0.1 \lesssim z \lesssim 1.7$. This improvement in our knowledge of the luminosity distances of SNe-Ia will provide a much stronger test of the Λ CDM model.

7. Number Counts

Counting galaxies or clusters of galaxies as a function of their redshift seems to be a very promising way to test different cosmological models (Huterer & Turner 2001; Podariu & Ratra 2001). The idea behind this procedure is that once we know, either by analytic calculations or by numerical simulations, the evolution of the comoving (i.e., coordinate) density of a given class of objects (e.g., galaxies or clusters of galaxies), counting the observed number of such objects, per unit solid angle as a function of their redshift, is equivalent to tracing back the area of the Universe at different stages that we can observe today. In other words, it is equivalent to determining our past light cone by constructing it from the area of these observed spherical sections of the Universe, parametrized by their redshift. Since this

⁶<http://snap.lbl.gov/>

light cone is very sensitive to the underlying cosmological model, number counts provide a valuable tool for testing the mechanism which accounts for the accelerated expansion of the Universe.

This kind of test was first performed using galaxies brighter than certain (apparent) magnitudes by Loh & Spillar (1986), with the simplified assumptions that the comoving density of galaxies is constant and that their luminosity function retains similar shape over the redshift range $0.15 \lesssim z \lesssim 0.85$. Using the photometric redshift of 406 galaxies in that range, they were able to measure the ratio of the total energy density in the Universe to the critical density, obtaining $\Omega_0 = 0.9_{-0.5}^{+0.6}$. However, the validity of Loh & Spillar’s assumptions is still not clear due to the lack, to the present, of a complete theory of galaxy formation and evolution. In order to circumvent this problem, Newman & Davis (2000) then suggested that galaxies having the same circular velocity may be regarded as good candidates for number count tests, since the evolution of the comoving number density of dark halos having a given circular velocity can be calculated by a semi-analytic approach. Moreover, they claim, the comoving abundance of such objects at redshift $z \approx 1$ (relative to their present abundance) is very insensitive to the underlying cosmological model (under reasonable matter power spectrum assumptions). Other objects that one can count are clusters of galaxies (Bahcall & Fan 1998; Blanchard & Bartlett 1998; Viana & Liddle 1999; Haiman, Mohr, & Holder 2001; Newman et al. 2002), which are simpler objects than galaxies, in the sense that their formation and evolution, and therefore their density, depend mostly on well-understood gravitational physics.

Whatever class of objects one uses to perform the number count test, a key ingredient one needs to provide as an input, as stressed above, is the evolution of their comoving density,

$$n_c(z) \equiv \frac{\sqrt{1 - kr^2} dN(z)}{r^2 dr d\Omega} , \quad (50)$$

where $d\Omega \equiv \sin\theta d\theta d\phi$ is the solid-angle element and $dN(z)$ is the number of such objects, at the spatial section at redshift z , contained in the coordinate volume $r^2 dr d\Omega / \sqrt{1 - kr^2}$. In order to find out the number of objects, per unit solid angle, with redshift between z and $z + dz$, we have to use the fact that the objects we are observing today with redshift z possess coordinate r which satisfies the past light-cone equations (45) and (46). Thus, by making use of these equations to eliminate the explicit radial dependence in equation (50), we get the number of observed objects with redshift between z and $z + dz$, per unit solid angle:

$$\frac{dN}{dz d\Omega}(z) dz = \begin{cases} n_c(z) (a_0 H_0)^{-3} E(z)^{-1} \left(\int_0^z E(z')^{-1} dz' \right)^2 dz & , k = 0 \\ n_c(z) (a_0 H_0)^{-3} E(z)^{-1} \left[\Omega_{k0}^{-1/2} \sinh \left(\Omega_{k0}^{1/2} \int_0^z E(z')^{-1} dz' \right) \right]^2 dz & , k \neq 0 \end{cases} , \quad (51)$$

with $E(z) \equiv H(z)/H_0$.

In order to illustrate number counts predicted by the VCDM cosmological model, in figure 4 we plot $dN(z)/dzd\Omega$ given by equation (51), with $H(z)$ given by equation (47). Then, we apply the resulting formula to the spatially flat case and use the parameters obtained in section 5 adopting the HST-Key-Project constraint (see fig. 2), namely $\Omega_{m0} = 0.34_{-0.14}^{+0.08}$. Also, we follow Podariu & Ratra (2001) and Loh & Spillar (1986) in assuming, for simplicity, the constancy of the comoving density, $n_c(z) = n_0 a_0^3$ (n_0 is the *proper* density at the present epoch). For sake of comparison, we also plot the spatially flat Λ CDM prediction, with $\Omega_{\Lambda 0} = 0.67$ and the same assumption of constant density. Obviously, the predictions could be improved by dropping this latter assumption and taking into account the density evolution of the observed objects, as mentioned earlier. However, calculating such evolution is beyond the scope of the present paper, not to mention the fact that it is still not completely clear which class of objects we should choose. Moreover, once a more precise $n_c(z)$ is known, it is a simple task to take it into account since $dN(z)/dzd\Omega$ is simply proportional to $n_c(z)$. From figure 4 we see that the VCDM model predicts more objects to be observed over redshifts $z \lesssim 2$ than the Λ CDM model. In fact, in a small redshift interval $\Delta z \ll 1$ around $z \approx 1$ the VCDM model predicts approximately 30% more objects than the Λ CDM model for approximately the same value of Ω_{m0} (and the same value of n_0/H_0^3). Note that this last conclusion should also hold for the counts of galaxies at fixed circular velocities suggested by Newman & Davis (2000), since their comoving density, even though not constant, is very insensitive to the underlying cosmological model at $z \approx 1$. We did not mention here the presence of selection effects, since they highly depend on the measurement procedure itself. Notwithstanding, these effects may also be included in the computation via an “effective” $n_c(z)$, which then should be viewed as the number of objects at the spatial section with redshift z , per comoving volume, satisfying the detectability conditions.

Measurements of $dN/dzd\Omega$ will provide a valuable way to test the VCDM cosmological model and distinguish it from the Λ CDM model, when combined with CMBR anisotropy results. Such measurements will soon become available, as the DEEP (Deep Extragalactic Evolutionary Probe) Redshift Survey⁷ expects to complete its measurements of the spectra of approximately 65,000 galaxies in the redshift range $0.7 \lesssim z \lesssim 1.5$ by the year 2004.

⁷<http://deep.ucolick.org/>

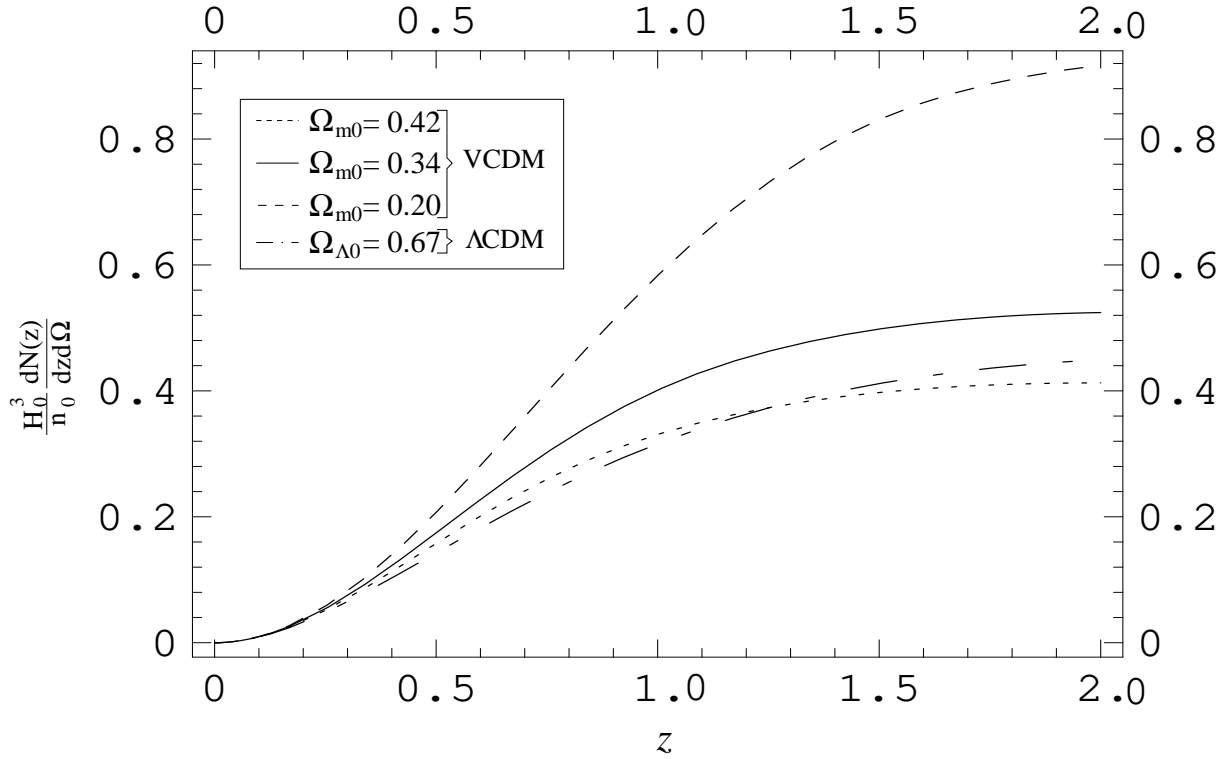


Fig. 4.— Plot of the predicted number counts of objects per redshift interval and per solid angle, $dN(z)/dzd\Omega$ (normalized by the present number of such objects in the volume H_0^{-3}) as functions of their redshift z , for the spatially flat VCDM (with $\Omega_{m0} = 0.34^{+0.08}_{-0.14}$) and Λ CDM (with $\Omega_{\Lambda 0} = 0.67$) models. In this plot, the comoving density is assumed to be constant.

8. Vacuum Equation of State

The dark-energy equation of state $\rho_v = \rho_v(p_v)$ in the VCDM cosmological model with $k = \pm 1$ or 0 can be easily obtained, for $t > t_j$, from equations (29) and (30):

$$\rho_v = 3p_v + \frac{\bar{m}^2}{8\pi G} \left[1 - \left(1 + \frac{32\pi G}{\bar{m}^2} p_v \right)^{3/4} \right]. \quad (52)$$

Moreover, from the same pair of equations we also obtain the ratio $w \equiv p_v/\rho_v$ as a function of redshift:

$$\begin{aligned} w(z) &= \frac{\zeta^4 - 1}{3\zeta^4 - 4\zeta^3 + 1} \\ &= \frac{\zeta^3 + \zeta^2 + \zeta + 1}{3\zeta^3 - \zeta^2 - \zeta - 1}, \quad 0 < \zeta < 1, \end{aligned} \quad (53)$$

where $\zeta \equiv a_j/a = (1+z)/(1+z_j)$. Note that equations (29), (30), (52), and (53) are the same as the respective ones presented by Parker & Raval (2001) in dealing with the spatially flat VCDM model. (Note, however, that the spatial curvature changes the value of z_j ; see eqs. [22] and [16].)

In figure 5 we plot the redshift dependence of the ratio w , given by equation (53), for the spatially flat VCDM model using the cosmological parameters obtained in section 5 adopting the HST-Key-Project constraint. The present value of this ratio, $w_0 \equiv w(z=0)$, using $\Omega_{m0} = 0.34_{-0.14}^{+(0.46;0.08)}$, is $w_0 = -1.28_{+0.12}^{-(0.91;0.08)}$. Note, from the expression for $w(z)$, that $w \rightarrow -\infty$ as $z \rightarrow z_{j-}$, which is simply a consequence of the previously mentioned fact that the vacuum energy approaches a negligibly small value (more rapidly than the vacuum pressure) as $z \rightarrow z_{j-}$. That no drastic consequence follows from the divergence of w is evident from figure 6, where we plot, using equations (33) and (36), the ratio $w_{\text{tot}} \equiv p/\rho$ between the *total* pressure p and the *total* energy density ρ present in the Universe, as a function of redshift. For the sake of comparison, we also plot in the same figure the correspondent ratio $w_{\text{tot}}^{(\Lambda)}$ given by the spatially flat Λ CDM model,

$$\begin{aligned} w_{\text{tot}}^{(\Lambda)} &= \frac{p_r + p_\Lambda}{\rho_r + \rho_m + \rho_\Lambda} \\ &= \frac{(\Omega_{r0}/3)(1+z)^4 - \Omega_{\Lambda0}}{\Omega_{r0}(1+z)^4 + (1 - \Omega_{r0} - \Omega_{\Lambda0})(1+z)^3 + \Omega_{\Lambda0}}, \end{aligned} \quad (54)$$

with $\Omega_{\Lambda0} = 0.67$ and $\Omega_{r0} = 8.33 \times 10^{-5}$. In the VCDM model note that for times earlier than t_j (i.e., $z > z_j$), during the matter dominated era, the total energy density, $\rho \approx \rho_m$, and the total pressure, $p = \rho_r/3$, lead to a negligible value of the ratio w_{tot} . After t_j ($z < z_j$), the negative pressure of the vacuum grows very rapidly in magnitude, becoming dominant and

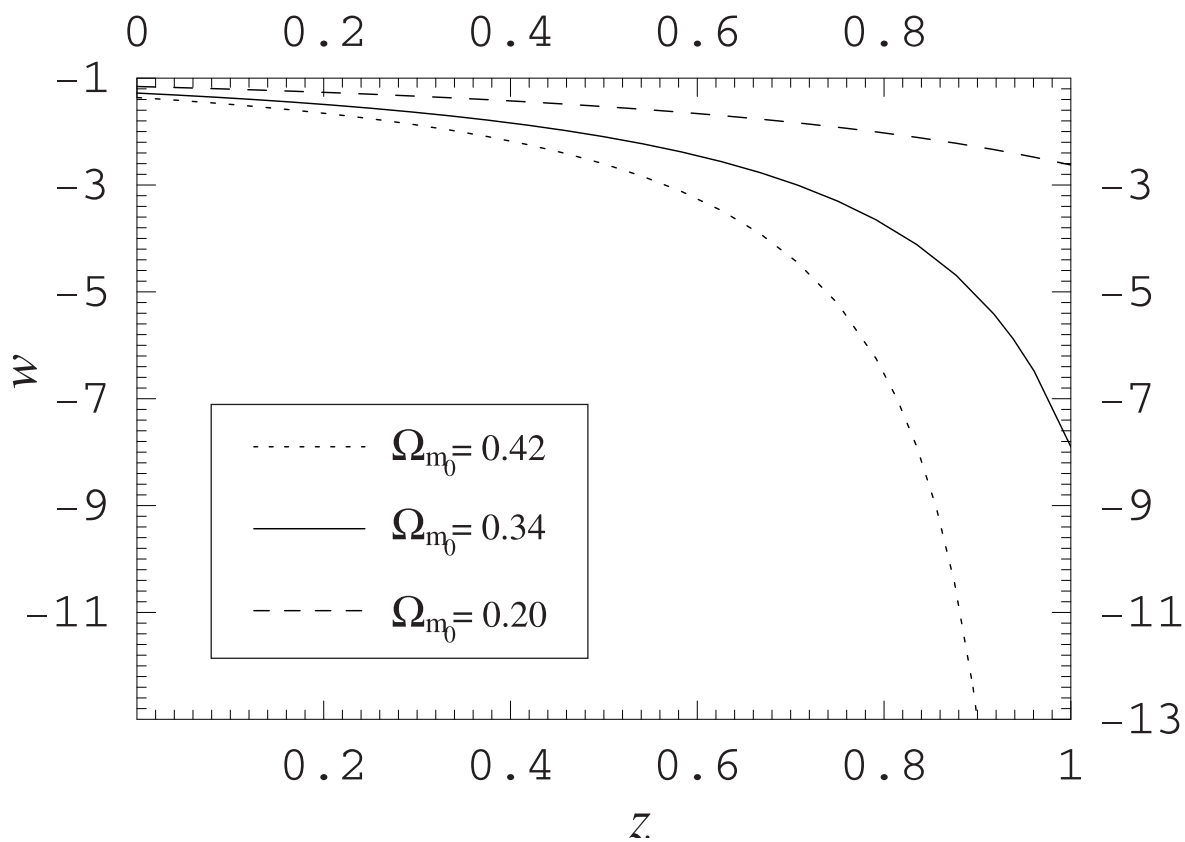


Fig. 5.— Plot of the predicted ratio $w \equiv p_v/\rho_v$ as a function of redshift z , for the spatially flat VCDM model with $\Omega_{m_0} = 0.34^{+0.08}_{-0.14}$ (the HST-Key-Project constraint was adopted). The present value of such ratio is $w_0 = -1.28^{+0.08}_{-0.12}$. Moreover, $w \rightarrow -\infty$ as $z \rightarrow z_{j-} = (1.19^{+0.19}_{-0.47})_-$

determining a very sharp transition to the dark-energy dominated era. This is an important distinction between the VCDM (i.e., vacuum metamorphosis) model and the Λ CDM model, which presents a rather gradual transition (see fig. 6).

In order to analyze not only the value of w but also its rate of change in redshift, we plot in figure 7, using $\Omega_{m0} = 0.34$, the curve $(w(z), w'(z))$, where $w'(z) \equiv dw(z)/dz$. The redshift z is used as the parameter of the curve. The present value $w'_0 \equiv w'(z=0)$ predicted by the spatially flat VCDM model is $w'_0 = -0.8_{+0.4}^{-(4.2;0.3)}$. Note that $w \rightarrow -1$ and $w' \rightarrow 0$ as $z \rightarrow -1$, which means that in the asymptotic future (assuming that nothing new will prevent the unbounded expansion of the Universe) the dark energy of the VCDM model behaves like an effective cosmological constant, with value given by $\Lambda_{\text{eff}} \equiv \bar{m}^2/4 = 5.1_{+2.1}^{-(3.2;0.4)} \times 10^{-66} \text{ eV}^2$. For comparison, in a Λ CDM model with $H_0 \approx 65 \text{ km s}^{-1} \text{ Mpc}^{-1}$ and $\Omega_{\Lambda 0} \approx 0.67$, one would have $\Lambda = 3\Omega_{\Lambda 0}H_0^2 \approx 3.8 \times 10^{-66} \text{ eV}^2$.

The experimental determination of $w(z)$, avoiding model-dependent assumptions, relies basically on measurements that, at least in principle, will determine $H(z)$ with sufficient precision to provide also a reliable determination of $H'(z) \equiv dH(z)/dz$ (Huterer & Turner 2001). To see this, let us consider the conservation equation satisfied by the total energy density ρ and the total pressure p , namely $d(\rho a^3) + p d(a^3) = 0$. Thus, with the (only) assumption that matter and radiation are separately conserved, we have that the energy density, ρ_X , and pressure, p_X , of dark energy (whatever it is) also satisfy the same conservation equation, which implies

$$\frac{1}{\rho_X} \frac{d\rho_X}{dz} = -\frac{(1+w_X)}{a^3} \frac{d(a^3)}{dz} = 3 \frac{(1+w_X)}{(1+z)}, \quad (55)$$

where $w_X \equiv p_X/\rho_X$ and we have used $1+z = a_0/a$. Considering the general expression for the Hubble parameter as a function of redshift (which is obtained from Einstein's equation together with the assumption of separate conservation of matter and radiation),

$$\frac{H(z)^2}{H_0^2} = \Omega_{r0}(1+z)^4 + \Omega_{m0}(1+z)^3 + \Omega_{k0}(1+z)^2 + \Omega_{X0} \frac{\rho_X(z)}{\rho_{X0}} \quad (56)$$

[with ρ_{X0} being the present value of the dark-energy density and $\Omega_{X0} \equiv 8\pi G\rho_{X0}/(3H_0^2)$], and using it and its redshift derivative to evaluate the left-hand-side of equation (55), we finally obtain the desired expression for $w_X(z)$:

$$\begin{aligned} w_X(z) &= \frac{(1+z)}{3} \frac{[d\rho_X(z)/dz]}{\rho_X(z)} - 1 \\ &= \frac{1}{3} \frac{[2(1+z)E'(z) - 3E(z)] E(z) - (1+z)^2 [\Omega_{r0}(1+z)^2 - \Omega_{k0}]}{E(z)^2 - \Omega_{r0}(1+z)^4 - \Omega_{m0}(1+z)^3 - \Omega_{k0}(1+z)^2}, \end{aligned} \quad (57)$$

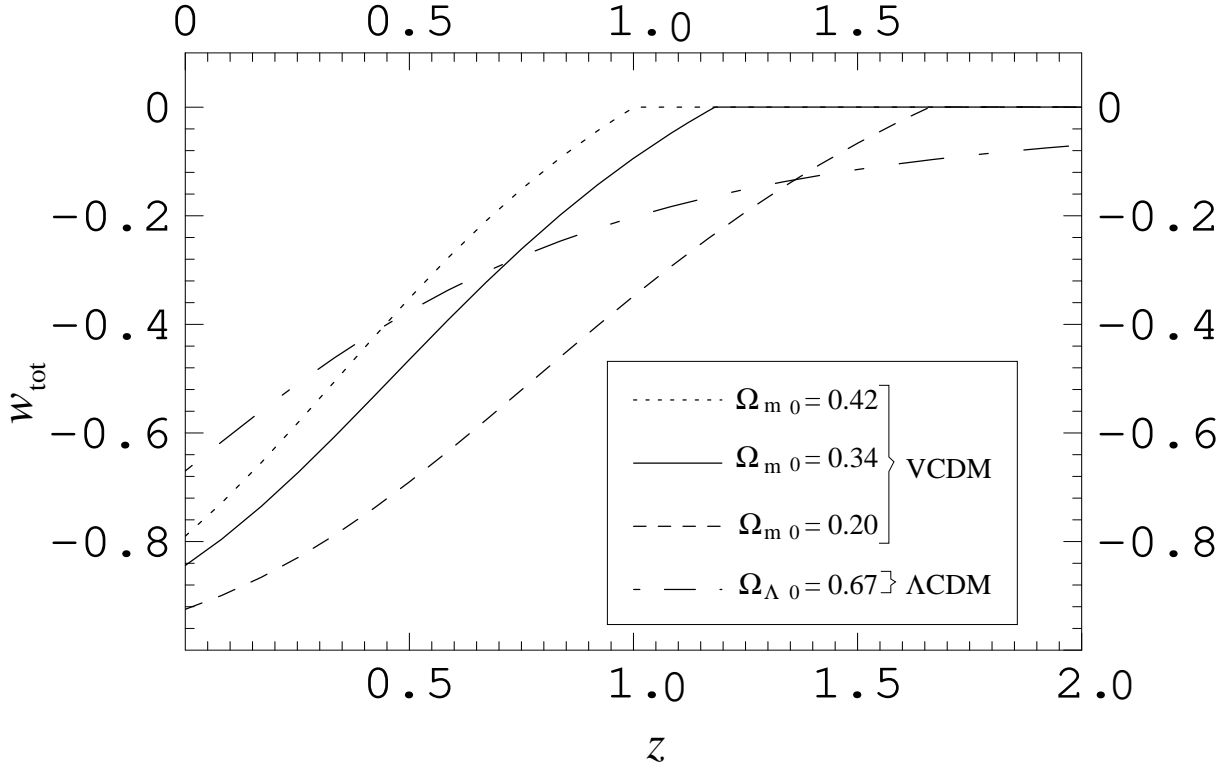


Fig. 6.— Plot of the ratio $w_{\text{tot}} \equiv p/\rho$ as a function of redshift z , for the spatially flat VCDM model with $\Omega_{m0} = 0.34^{+0.08}_{-0.14}$ and for the spatially flat Λ CDM model with $\Omega_{\Lambda0} = 0.67$. With these parameters, the present values of w_{tot} and $w_{\text{tot}}^{(\Lambda)}$ are $w_{\text{tot}}(z = 0) = -0.85^{+0.06}_{-0.07}$ and $w_{\text{tot}}^{(\Lambda)}(z = 0) = -0.67$. Note that for the VCDM model the ratio w_{tot} is negligible for times earlier than t_j (i.e., $z > z_j$), during the matter dominated era.

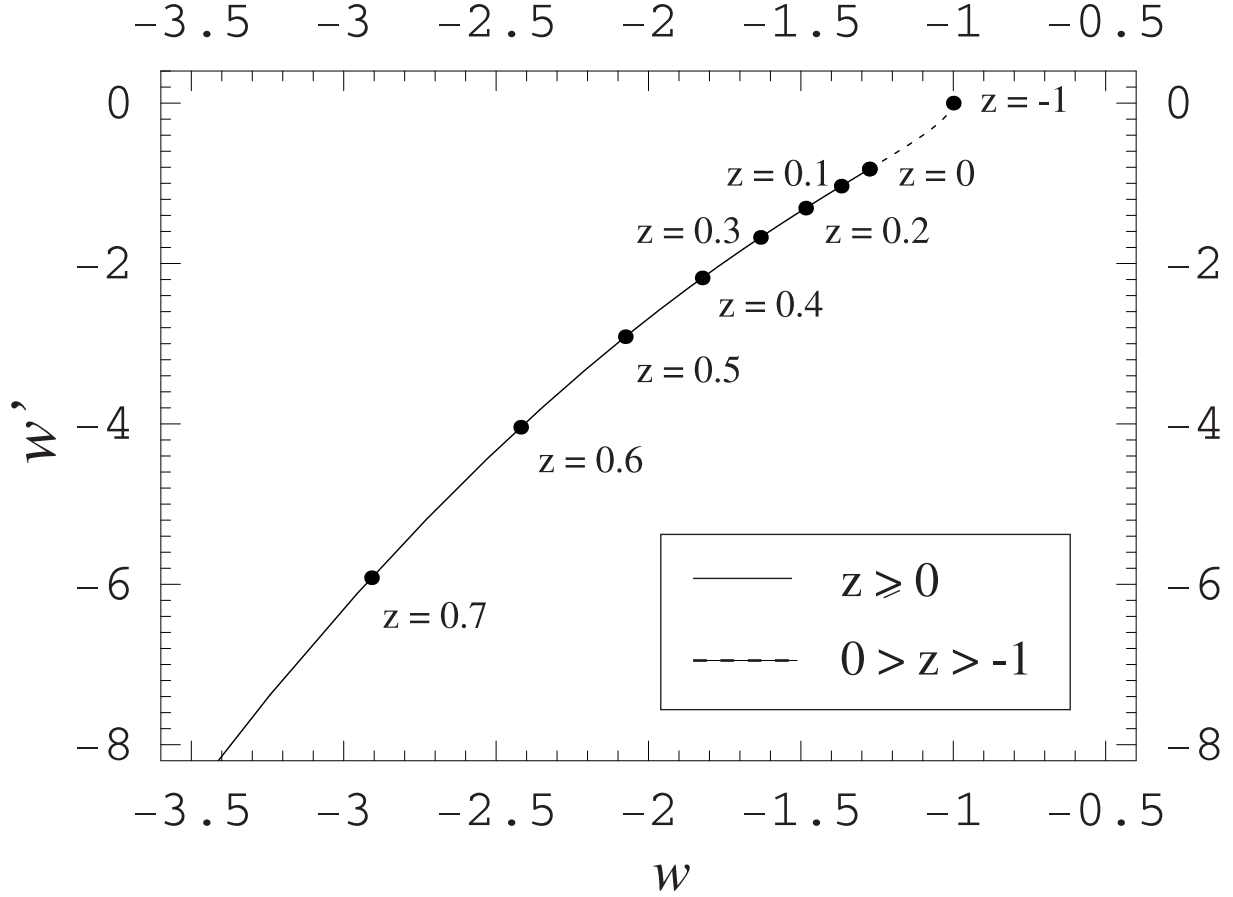


Fig. 7.— Plot of the curve $(w(z), w'(z))$, parametrized by the redshift z , for the spatially flat Λ CDM model with $\Omega_{m0} = 0.34$. The solid-line curve corresponds to redshift $z \geq 0$ while the dashed-line one corresponds to $-1 < z < 0$. At the present epoch we have $(w_0, w'_0) = (-1.28, -0.8)$. Note that $(w(z), w'(z)) \rightarrow (-1, 0)$ as $z \rightarrow -1$, which means that the dark energy of the Λ CDM model behaves like a cosmological constant in the asymptotic future.

where, again, $E(z) \equiv H(z)/H_0$ and $E'(z) \equiv dE(z)/dz$. Thus, as stated above, $w_X(z)$ can be found from the determination of $H(z)$ and $H'(z)$. The quantity $H(z)$ can be determined from the direct observables $d_L(z)$ and $dN(z)/dzd\Omega$, and the quantity $n_c(z)$ (Huterer & Turner 2001). This is done by using equation (45) to express the derivative with respect to r in equation (50) in terms of a derivative with respect to z , and then using equation (48) to express $r(z)$ in terms of $d_L(z)$. This leads to the following expression for $H(z)$:

$$H(z) = \frac{n_c(z)}{a_0^3} \left(\frac{dN(z)}{dzd\Omega} \right)^{-1} \frac{d_L(z)^2}{(1+z)^2}. \quad (58)$$

Thus, by considering measurements of luminosity distances and number counts, $H(z)$ can be regarded as a directly observable quantity, which gives $w_X(z)$ through equation (57). In this sense, future data provided by the proposed satellite SNAP on supernovae luminosity distances (see sec. 6) and by the DEEP redshift survey on number counts (see sec. 7) may greatly improve our knowledge of the dark-energy equation of state.

9. Conclusion

We have shown that the current observational data indicating that the expansion of the Universe is undergoing acceleration are quite consistent with the hypothesis that a transition to a constant-scalar-curvature stage of the expansion occurred at a redshift $z \sim 1$ in the spatially flat FRW universe having zero cosmological constant. This is the scenario proposed in the VCDM (or vacuum metamorphosis) model introduced by Parker and Raval. The late constancy of the scalar curvature at a value $R_j = \bar{m}^2$ is induced by quantum effects of a free scalar field of low mass in the curved cosmological background. The parameter \bar{m} , related to the mass of the field, is the only new relevant parameter introduced in this model, and can be expressed in terms of the present cosmological parameters H_0 , Ω_{m0} , Ω_{r0} , and Ω_{k0} (see eq. [16]).

Comparison of the CMBR-power-spectrum data with the flat-VCDM-model prediction, without or with the HST-Key-Project result as a constraint (see figs. 1 and 2, and table 1), gives the values of the cosmological parameters to be $H_0 = 65_{+10}^{-(16;1)} \text{ km s}^{-1} \text{ Mpc}^{-1}$ and $\Omega_{m0} = 0.34_{-0.14}^{+(0.46;0.08)}$. (Recall the definition of our notation in sec. 2: the uncertainties appearing in parenthesis refer to the 95% confidence level, without and with the HST constraint, respectively.) Such values lead to $\bar{m} = 4.52_{+0.84}^{-(1.76;0.18)} \times 10^{-33} \text{ eV}$, and the best-fit values from the CMBR data give rise to a very good no-parameter fit to the SNe-Ia observational data. However, the SNe-Ia data are not accurate enough to draw a clear distinction between the VCDM and Λ CDM models. Other quantities of interest predicted by the VCDM model with the cosmological parameters mentioned above are the time and redshift at the transition

between the matter-dominated and constant-scalar-curvature stages, ($t_j = 5.33_{-0.84}^{+3.41;0.22}$ Gyr and $z_j = 1.19_{+0.47}^{-(0.76;0.19)}$), the time and redshift when the accelerated expansion started ($t_a = 8.0_{-1.2}^{+(5.2;0.4)}$ Gyr and $z_a = 0.67_{+0.35}^{-(0.59;0.15)}$), and the age of the Universe, $t_0 = 14.9 \mp 0.8$ Gyr.

Regarding future tests of the VCDM model, we have presented the prediction of number counts as a function of redshift, and compared it with the analogous Λ CDM prediction (see fig. 4). For approximately the same cosmological parameters, the VCDM model predicts nearly 30% more objects to be observed in a small redshift interval around $z \approx 1$ than the Λ CDM model. Data provided by the DEEP Redshift Survey in the near future will likely be able to distinguish these two models. Also, DEEP data combined with future measurements of SNe-Ia luminosity distances provided by the proposed SNAP satellite should greatly improve our knowledge of the dark energy equation of state, which bears the most distinct feature of the VCDM model: $w < -1$ and $w' < 0$ (see figs. 5 and 7).

It should be noted that we have here considered the simplest form of the VCDM model, in which the transition to constant scalar curvature is continuous and effectively instantaneous (see fig. 6). This form of the model makes definite predictions regarding the distance moduli of SNe-Ia and number counts. Thus, it is encouraging that it remains a viable model when confronted with the current observational data. Other natural parameters that may come into the VCDM model are the time interval over which the transition occurs, and the vacuum expectation value of the scalar field. A nonzero value of the transition time interval would mainly affect the predictions around $z \sim 1$, and a nonzero value of the vacuum expectation value is likely to increase the ratio of pressure to density, w . Future observational data will determine if it is necessary to consider nonzero values for these parameters.

This work was supported by NSF grant PHY-0071044 and Wisconsin Space Grant Consortium. The authors thank Koji Uryu for helpful comments and suggestions on the figures, and Alpan Raval for helpful discussions.

REFERENCES

- Abramo, L. R., Tsamis, N. C., & Woodard, R. P. 1999, Fortsch. Phys., 47, 389
- Abroe, M. E., et al. 2001, MNRAS, in press (astro-ph/0111010)
- Armendariz-Picon, C., Mukhanov, V., & Steinhardt, P. J. 2001, Phys. Rev. D, 63, 103510
- Bahcall, N. A., & Fan, X. 1998, ApJ, 504, 1

- Bassett, B. A., Kunz, M., Silk, J., & Ungarelli, C. 2002a, MNRAS, in press (astro-ph/0203383)
- Bassett, B. A., Kunz, M., Silk, J., & Ungarelli, C. 2002b, preprint (astro-ph/0205428)
- Bean, R., Hansen, S. H., & Melchiorri, A. 2002, Nucl. Phys. Proc. Suppl., 110, 167
- Blanchard, A., & Bartlett, J. G. 1998, A&A, 332, L49
- Bond, J. R., Jaffe, A. H., & Knox, L. E. 2000, ApJ, 533, 19
- Caldwell, R., Dave, R., & Steinhardt, P. J. 1998, Phys. Rev. Lett., 80, 1582
- Caldwell, R. 2002, Phys. Lett. B, 545, 23
- Colberg, J. M., et al. 2000, MNRAS, 319, 209
- DeWitt, B. S. 1965, Dynamical Theory of Groups and Fields (New York: Gordon and Breach)
- Dodelson, S., Gates, E., & Turner, M. S. 1996, Science, 274, 69
- Dodelson, S., Kaplinghat, M., & Stewart, E. 2000, Phys. Rev. Lett., 85, 5276
- Dolgov, A. D. 1983, in The Very Early Universe, ed. G. W. Gibbons, S. W. Hawking, and S. T. C. Siklos (Cambridge: Cambridge University Press)
- Durrer, R., Novosyadlyj, B., & Apunevych, S. 2001, ApJ, submitted (astro-ph/0111594)
- Ford, L. H. 1987, Phys. Rev. D, 35, 2339
- Ford, L. H. 2002, preprint (gr-qc/0210096)
- Freedman, W. L., et al. 2001, ApJ, 553, 47
- Haiman, Z., Mohr, J. J., & Holder, G. P. 2001, ApJ, 553, 545
- Hu, W., Fukugita, M., Zaldarriaga, M., & Tegmark, M. 2001, ApJ, 549, 669
- Huterer, D., & Turner, M. S. 2001, Phys. Rev. D, 64, 123527
- Jack, I., & Parker, L. 1985, Phys. Rev. D, 31, 2439
- Jackiw, R. 1974, Phys. Rev. D, 9, 1686
- Knox, L., Christensen, N., & Skordis, C. 2001, ApJ, 563, L95

- Krauss, L. M. 2000, *Phys. Rep.*, 333, 33
- Krauss, L. M., & Turner, M. S. 1995, *Gen. Rel. Grav.*, 27, 1137
- Loh, E. D., & Spillar, E. J. 1986, *ApJ*, 307, L1
- Masi, S., et al. 2002, preprint (astro-ph/0201137)
- Melchiorri, A., Mersini, L., Odman, C. J., Trodden, M. 2002, preprint (astro-ph/0211522)
- Netterfield, C. B., et al. 2002, *ApJ*, 571, 604
- Newman, J. A., & Davis, M. 2000, *ApJ*, 534, L11
- Newman, J. A., Marinoni, C., Coil, A. L., & Davis, M. 2002, *PASP*, 114, 29
- Ostriker, J. P., & Steinhardt, P. J. 1995, *Nature*, 377, 600
- Parker, L., & Toms, D. J. 1985a, *Phys. Rev. D*, 31, 953
- Parker, L., & Toms, D. J. 1985b, *Phys. Rev. D*, 31, 2424
- Parker, L., & Toms, D. J. 1985c, *Phys. Rev. D*, 32, 1409
- Parker, L., & Raval, A. 1999a, *Phys. Rev. D*, 60, 063512
- Parker, L., & Raval, A. 1999b, *Phys. Rev. D*, 60, 123502
- Parker, L., & Raval, A. 1999c, preprint (gr-qc/9908069)
- Parker, L., & Raval, A. 2000, *Phys. Rev. D*, 62, 083503
- Parker, L., & Raval, A. 2001, *Phys. Rev. Lett.*, 86, 749
- Peebles, P. J. E. 1993, *Principles of Physical Cosmology* (Princeton: Princeton University Press)
- Perlmutter, S., et al. 1998, *Nature*, 391, 51
- Perlmutter, S., et al. 1999, *ApJ*, 517, 565
- Podariu, S., & Ratra, B. 2001, *ApJ*, 563, 28
- Pryke, C., Halverson, N. W., Leitch, E. M., Kovac, J., Carlstrom, J. E., Holzzapfel, W. L., & Dragovan, M. 2002, *ApJ*, 568, 46
- Riess, A. G., et al. 1998, *AJ*, 116, 1009

- Riess, A. G., et al. 2001, *ApJ*, 560, 49
- Schwinger, J. 1951, *Phys. Rev.*, 82, 664
- Seljak, U., & Zaldarriaga, M. 1996, *ApJ*, 469, 437
- Tsamis, N. C., & Woodard, R. P. 1998a, *Phys. Lett. B*, 426, 21
- Tsamis, N. C., & Woodard, R. P. 1998b, *Phys. Rev. D*, 57, 4826
- Turner, M. S. 2001, *ApJ*, submitted (astro-ph/0106035)
- Viana, P. T. P., & Liddle, A. R. 1999, *MNRAS*, 303, 535
- Wang, X., Tegmark, M., & Zaldarriaga, M. 2002, *Phys. Rev. D*, 65, 123001
- Zaldarriaga, M., & Seljak, U. 2000, *ApJS*, 129, 431
- Zlatev, I., Wang, L., & Steinhardt, P. J. 1999, *Phys. Rev. Lett.*, 82, 896